


Increased expression of Trpv1 in peripheral terminals mediates thermal nociception in Fabry disease mouse model

Jarmila Lakomá, PhD¹, Roberto Rimondini, PhD², Antonio Ferrer Montiel, PhD³, Vincenzo Donadio, MD¹, Rocco Liguori, MD^{1,4} and Marco Caprini, PhD⁵

Molecular Pain
Volume 12: 1–16
© The Author(s) 2016
Reprints and permissions:
sagepub.co.uk/journalsPermissions.nav
DOI: 10.1177/1744806916663729
mpx.sagepub.com


Abstract

Fabry disease is a X-linked lysosomal storage disorder caused by deficient function of the alpha-galactosidase A (α -GalA) enzyme. α -GalA deficiency leads to multisystemic clinical manifestations caused by the preferential accumulation of globotriaosylceramide (Gb3) in the endothelium and vascular smooth muscles. A hallmark symptom of Fabry disease patients is neuropathic pain that appears in the early stage of the disease as a result of peripheral small fiber damage. The α -GalA gene null mouse model (α -GalA(-/0)) has provided molecular evidence for the molecular alterations in small type-C nociceptors in Fabry disease that may underlie their hyperexcitability, although the specific mechanism remains elusive. Here, we have addressed this question and report that small type-C nociceptors from α -GalA(-/0) mice exhibit a significant increase in the expression and function of the TRPV1 channel, a thermoTRP channel implicated in painful heat sensation. Notably, male α -GalA(-/0) mice displayed a \approx 2-fold higher heat sensitivity than wild-type animals, consistent with the augmented expression levels and activity of TRPV1 in α -GalA(-/0) nociceptors. Intriguingly, blockade of neuronal exocytosis with peptide DD04107, a process that inhibits among others the algescic membrane recruitment of TRPV1 channels in peptidergic nociceptors, virtually eliminated the enhanced heat nociception of α -GalA(-/0) mice. Together, these findings suggest that the augmented expression of TRPV1 in α -GalA(-/0) nociceptors may underly at least in part their increased heat sensitivity, and imply that blockade of peripheral neuronal exocytosis may be a valuable pharmacological strategy to reduce pain in Fabry disease patients, increasing their quality of life.

Keywords

Fabry disease, pain, small fiber neuropathy, α -GalA null mice, ion channels

Date received: 14 March 2016; revised: 13 June 2016; accepted: 7 July 2016

Introduction

Fabry disease (FD) is a X-linked lysosomal storage disorder caused by the deficient activity of α -galactosidase A (α -Gal A), encoded by the GLA gene (Xq22.1), which is responsible for the catabolism of neutral glycosphingolipids.¹ Deficient enzymatic activity results in the progressive intralysosomal deposition of glycosphingolipids, predominantly globotriaosylceramide (Gb3), in a variety of cell types, including capillary endothelial cells, renal (podocytes, tubular cells, glomerular endothelial, mesangial and interstitial cells), cardiac (cardiomyocytes and fibroblasts), smooth-muscle cells, and nerve cells.² Therefore, the consequence is the accumulation of the sphingolipid globotriaosylceramide (Gb3) in multiple

¹IRCCS Institute of Neurological Sciences, AUSL Bologna, Italy

²Department of Medical and Clinical Sciences (DIMEC), University of Bologna, Italy

³Institute of Molecular and Cellular Biology, University of Miguel Hernandez, Spain

⁴Department of Biomedical and Neuromotor Sciences (DIBINEM), University of Bologna, Italy

⁵Department of Pharmacy and Biotechnology (FaBiT), Laboratory of Human and General Physiology, University of Bologna, Italy

Corresponding author:

Marco Caprini, Department of Pharmacy and Biotechnology, Laboratory of Human and General Physiology, Via San Donato 19/2, Bologna 40127, Italy.
Email: m.caprini@unibo.it



organs, particularly in kidneys, heart, and the nervous system.³ The early manifestations of FD appear in childhood and usually include acroparesthesia, angiokeratomas, hypohidrosis and pain. Episodes of acute, agonizing pain, typically beginning in the extremities and radiating inward, may persist from minutes to several days, giving rise to the Fabry pain crisis.⁴ The first signs appear already in childhood and with age, severe complications cause considerable morbidity and premature death involving the kidneys, heart, and brain.^{5,6} It remains difficult to clearly define such a phenomenon as the pain. In medical conditions, pain is a symptom, a response to noxious stimuli, such as cold or heat, detected by peripheral damage-sensing neurons (nociceptors, peripheral terminals), mechanical stress or the chemical signals arising during inflammation. It is carried through small diameter nerve fibers to the central nervous system (CNS). Specifically, it has been demonstrated that FD patients show reduced intraepidermal nerve fiber density and altered thermal perception.⁷

The underlying molecular and functional mechanisms of pain in small fiber neuropathy patients with FD are still not completely understood, although a small fiber peripheral neuropathy affecting small unmyelinated and myelinated nerve fibers is frequently found.^{8,9} Pain in FD is assumed to be neuropathic because Gb3 deposits have been observed in dorsal root ganglia of Fabry patients.¹⁰⁻¹² Our first hypothesis, at the molecular level, was referred to the role of the Gb3 deposits in the cell bodies of cells as a typical feature of FD patients.^{13,14} Specifically, Gb3 accumulations would interfere with the function of cellular membrane proteins and receptors leading to a direct pathological effect on ganglia or axons of small peripheral sensory neurons in pain perception and/or transduction.¹⁴⁻¹⁶ In a previous study, we reported that α -GalA null mice displayed neuropathic pain evidenced by thermal hyperalgesia, mechanical allodynia, and histological analyses.¹² These findings suggested that this was a good model to study the peripheral small fiber neuropathy exhibited by FD and provide molecular evidence for the hyperexcitability of small nociceptors in FD. Notably, at the molecular level, the α -GalA(-/0) animals showed significant increase immunoreactivity of TRPV1 and Nav1.8, and a decrease immunoreactivity of TRPM8 ion channels in their cutaneous terminals.¹³ Thereafter, it has been suggested that the accumulation of elevated glycosphingolipids concentration in sensory neurons have a direct role in their enhanced excitability.¹⁷⁻¹⁹ Moreover, a modulatory effect of lyso-Gb3 on voltage-gated calcium currents has also been suggested in the same mouse model.²⁰

In the present study, we report that the α -Gal(-/0) male mice DRG exhibit molecular and structural alterations in painful heat sensation consistent with overexpression and enhanced activity of TRPV1 ion channel.

Blockade of TRPV1 neuronal exocytosis with peptide DD04107 results in attenuation of heat hypersensitivity. These findings provide a key suggestion to possible mechanism underlying the higher heat sensitivity of FD patients and suggest a therapeutic strategy for future treatment.

Materials and methods

Animal procedures

Heterozygous female mice for α -GalA gene deletion (α -GalA(+/-)), JAX strain *B6;129-Gla^{tm1Kul}/J* (stock number 003535), and wild-type (WT) male α -GalA(+/-) were purchased from Charles River Laboratories Italia SRL (Jackson Laboratory; Bar Harbor, ME). To obtain α -GalA(-/0) hemizygous male mice, we crossed the α -GalA(+/-) female and α -GalA(-/0) male mice. The mice were housed in groups of six in individually ventilated cages (Tecniplast, Italia) with water and food ad libitum in controlled environmental conditions: lights on from 7.00 a.m. to 7.00 p.m., $22 \pm 2^\circ\text{C}$ temperature and 65% humidity. For the results of this work, we used only males for both, α -GalA(-/0) and α -GalA(+/-) mice; because of the greater severity demonstrated in males, we decided to focus our study only on the animal model of WT and knockout (KO) males. Behavioral experiments were carried out at the Department of Medical and Clinical Sciences of the University of Bologna with the approval of the local ethical committee (Veterinary Service of the University of Bologna) and in agreement with the National Animal Welfare Act. All efforts were made to minimize animal suffering and the number of animals used was kept to a minimum by the experimental design. All the procedures followed in this work complied with the European Community Council Directive of 24 November 1986 (86/609/EEC) and were approved by the Ethical committee of the University of Bologna (prot. N.43.IX/9). The age of animals used for behavioral and immunohistochemistry experiments was in the range of 8 to 12 weeks.

Genotyping

Genomic DNA was extracted from tail biopsies and genotyping of α -GalA KO mice was as described before¹³ using polymerase chain reactions with three oligonucleotides: oIMR5947 5'-AGGTCCACAGC AAAGGATTG-3', oIMR5948 5'-GCAAGTTGCC TCTGACTTC-3', and oIMR7415 5'-GCCAGAGG CCACTTGTGTAG-3'. The primers amplified bands of 202 bp for α -GalA(-/-) and 295 bp for α -GalA(+/+). The polymerase chain reaction conditions: 94°C for 3 min, 35 cycles of 94°C for 30 s, 64°C for 1 min and 72°C for 1 min, final elongation at 72°C for 2 min.

Preparation of rat dorsal root ganglion neuron

Primary cultures of DRG neurons were prepared from adult 8 to 12 weeks males, according to previously described protocols with some modifications.²¹ The mice were anesthetized by Halothane prior to decapitation. All ganglia were removed from each mouse and transferred in ice-cold Dulbecco's Phosphate Buffered Saline (DPBS) 1× (Gibco) and next the roots were cut using micro dissecting scissors. After rinsing in Dulbecco's Modified Eagle Medium (DMEM) (Gibco), the ganglia were placed in DMEM containing 5000 U/mL type IV collagenase (Worthington) for 45–75 min at 37°C, 5% CO₂, washed twice by medium with Fetal bovine serum (FBS) and then gently dissociated mechanically with passages through 0.5 mm and 0.6 mm sterile needles. Cells were centrifuge for 10 min at low speed and then appropriately diluted in 1 mL of DMEM medium containing 10% FBS (Gibco), 50 ng/mL nerve growth factor (Gibco), and 1.5 µg/mL cytosine β-D-arabinofuranoside (AraC, Sigma). For electrophysiology experiments, single cell suspension was plated at concentration 5,000 cells/2 mL of growing medium on polylysine (Sigma) with Laminin (Gibco) precoated culture dishes. For whole protein extraction 60,000 cells/5 mL were plated onto polylysine precoated culture dishes. For immunocytochemistry, 15,000 cell/mL were plated onto 18 mm round glass coverslips, precoated with polylysine and laminin. Cell culture was maintained in a 37°C, 5% CO₂ incubator during different periods (for electrophysiology experiments, the cells were used within first four days after plating (Days in vitro [DIV]); for Western Blot (WB), analysis and immunocytochemistry was used the same period and in parallel the 6 DIV). Cells were maintained in DMEM, supplemented with 10% FBS in the presence of 50 ng/mL nerve growth factor and 1.5 µg/mL cytosine β-D-arabinofuranoside (AraC, Sigma) to reduce glial cell expression. Half volume of medium was changed every second day.

Immunohistochemistry

For the immunohistochemistry of skin biopsy, the males of each genotype were deeply anesthetized with Isoflurane, shaved on the back, and rectangular section of 5 mm × 5 mm from the middle of the back (on top of the spine) was trimmed using a scalpel. In this manner, we reached a good view of the interfollicular epidermis as well as the hair follicles in the sagittal sections. We placed the piece of skin on Whatman filter paper (dermis side down) and fixed it in 4% paraformaldehyde (Sigma) rinsed in phosphate-buffered saline (PBS) (0.01 M, pH 7.4) at 4°C for three days. After fixation, we replaced the fixative solution with cryoprotective solution of 30% sucrose (Sigma). The skin biopsies were mounted in Tissue Tek OCT compound, frozen

and cryosectioned at 50 µm parallel to spine axis orientation (longitudinal free-floating sections). The immunohistochemistry of floating sections was processed in separated chambers for each genotype, reaching the same conditions for all three animals. The number of immunohistochemistry experiments was three and the total number of used animals was three for WT and three for KO. Sections were blocked with 5% bovine serum albumin (BSA) (Sigma) rinsed in PBS (0.01 M, pH 7.4) with 0.5% of triton X-100 (Sigma) for 1 h at room temperature, followed by incubation overnight with primary antibody rabbit anti-pan-neuronal marker PGP9.5 (1:1000; Serotec, Raleigh, NC) in 1% BSA rinsed in PBS (0.01 M, pH 7.4) with 0.5% of Triton X-100 at 4°C. After washing, they were incubated with secondary antibody Cy3-donkey anti-rabbit (1:200, Jackson ImmunoResearch) in 1% BSA rinsed in PBS (0.01 M, pH 7.4) with 0.05% of Triton X-100 for 2 h at room temperature. Finally, the sections were mounted into Fluoromount-G mounting medium containing DAPI (4',6-diaminobenzididine-2-phenylindole, dilactate, Sigma). Experimental, negative control samples were processed in parallel in different reaction chambers, without incubation with primary antibody. The fluorescent signal of negative control sample was taken as a threshold for fluorescent signal of experimental samples.

Cryosections of whole DRGs

Samples of whole DRG were isolated from 8- to 10-week-old animals and immediately fixed in 4% paraformaldehyde (Sigma) rinsed in PBS (0.01 M, pH 7.4) at 4°C for three days. After the fixation, we replaced the fixative solution with cryoprotective solution of 30% sucrose (Sigma). The spinal cord and DRG were cut into 10 and 20 µm sections, respectively. The 20 µm sections were incubated with hematoxylin and eosin staining solutions, and the 10 µm were incubated with rabbit anti-TRPV1 (1:50, Santa Cruz) and mouse anti-NeuN (1:2000, Millipore) overnight at 4°C in 1% BSA with 0.05% of Triton, then incubated with Cy2-donkey anti-mouse and Cy3-donkey anti-rabbit (1:200, from Jackson ImmunoResearch) for 2 h at T_{room} in dark. DAPI (dilactate; 300 nM, Invitrogen) was used for counterstaining. Images were taken by a confocal microscope.

Immunocytochemistry

DRG neurons of different time of growth (from 3 to 12 DIV) were fixed for 20 min with 4% paraformaldehyde (Sigma) rinsed in PBS (0.01 M, pH 7.4) at room temperature, followed by washes with PBS, blocking in 5% BSA (Sigma) with 0.5% of triton (Sigma), and incubation with primary antibodies overnight at 4°C in 1% BSA with 0.05% of Triton. Following day, the primary antibodies

were washed out by $1 \times$ PBS and followed by incubation with Cy2, Cy3-conjugated secondary antibodies (Jackson ImmunoResearch) for 2 h at T_{room} in dark.

Primary antibodies: goat anti-Nav1.8 (1:50, Santa Cruz),²² rabbit anti-TRPV1 (1:50, Santa Cruz),^{23–25} rabbit anti-TRPM8 (1:50, Santa Cruz), rat anti-CD77 (1:10, Abcam),²⁶ mouse anti-NeuN (1:2000, Millipore),²⁷ and rabbit anti-Tuj1 (β 3 Tubulin, 1:50, Santa Cruz).²⁸

Secondary antibodies: Cy2-donkey anti-rabbit, Cy2-donkey anti-mouse, Cy3-donkey anti-rat, and Cy3-donkey anti-rabbit (1:200, all from Jackson ImmunoResearch). DAPI (dilactate; 300 nM, Invitrogen) was used for counterstaining.

Western blot

Protein extracts were prepared from DRG neurons of different time of growth (from 3 to 6 DIV) homogenized with of lysis buffer (50 mM TRIS-HCl, pH 7.4, 100 mM NaCl, 1 mM PMSF, 1 mM EDTA, 5 mM Iodacetamide, 1% Triton X-100, 0.5% Sodium Dodecylsulfate). The extracts were sonicated for 10 min in 20 s intervals every 2 min and pelleted for 30 min at 12,000 r/min. The supernatant was collected and used to determine the protein content using the Bradford method.

Tissue lysates (40–80 g) were separated by 7.5%–10% SDS-polyacrylamide gel and transferred to hybond-ECL nitrocellulose membrane (Amersham). After transfer, the membrane was blocked by 5% BSA in PBS (0.01 M, pH 7.4) with 0.05% Tween 20 (Sigma) (PBST) for 1 h at room temperature. The membrane was incubated with primary antibodies against specific ionic channels goat anti-Nav1.8 (1:200, Santa Cruz), rabbit anti-TRPV1 (1:250, Immunological Sciences), rabbit anti-TRPM8 (1:100; Santa Cruz), and rabbit anti-actin (1:200, Sigma) in 1% BSA in PBST overnight at 4°C. The membrane was rinsed three times with PBST, each for 15 min and secondary antibody horseradish peroxidase-coupled secondary anti-rabbit (1:2000, Santa Cruz) and anti-goat (1:5000, Sigma) were employed for incubation in 1% BSA rinsed in PBST for 2 h at T_{room} . After washout of secondary-HRP binding antibody, the membrane was incubated with chemiluminescence substrate (Santa Cruz) for 5 min; protein bands were visualized on X-ray (Thermo Scientific). The intensity of the protein bands for all observed ICs (TRPV1, Nav1.8, and TRPM8) was quantified and normalized to the intensity of β -actin bands using the ImageJ software.

Evaluation of epidermal nerve fiber density in mice skin biopsy

The epidermal nerve fiber density identified by PGP 9.5 positive staining was calculated per linear millimeter of

epidermis.²⁹ The images of PGP9.5 positive immunostaining of mice skin biopsy acquired with 40 \times objective were analyzed using the ImageJ software. Only the neuronal fibers within the epidermis were taken into account. The total number of counted neuronal fibers was related to the final length of dermal/epidermal border.

Evaluation of TRPV1 expressing neuronal population in whole DRG sections

The total number of NeuN and/or TRPV1 positive cells was counted in 27 randomly chosen images, taken as Z-stack on Nikon confocal microscope. The ratio of TRPV1 expressing neurons per whole neuronal population (total number of neurons) for each genotype was calculated and represented as a percentage.

Electrophysiology

Salts and other chemicals were of the highest purity grade (Sigma-Aldrich). Cells were visualized with a phase-contrast inverted microscope (Nikon Italy, Firenze, Italy).

Voltage-clamp experiments were performed at room temperature (20°C–22°C) with the whole-cell configuration of the patch clamp technique.³⁰ DRG neurons were bathed in extracellular solution containing (in mM): 140 NaCl, 4 KCl, 2 CaCl₂, 2 MgCl₂, 10 HEPES, 5 Glucose, pH 7.4 with NaOH (320 mOsm/Kg with mannitol). To measure cationic currents, DRG were perfused with extracellular solution containing (in mM): 140 NaCl, 4 CsCl, 1 MgCl₂, 2 CaCl₂, 10 HEPES, 10 Glucose, pH 7.4 with CsOH (320 mOsm/Kg). The pipette solution contained (in mM): 140 CsCl, 1 MgCl₂, 5 EGTA, 10 HEPES, 10 mM Glucose, 3 mM ATP, pH 7.2 with CsOH (290 mOsm). The osmolality of all solutions was measured with a vapor-pressure osmometer (Wescor 5500, Delcon Italy). Patch pipettes were prepared from thin-walled borosilicate glass capillaries to have a tip resistance of 2–10 M Ω when filled with the pipette solution. Membrane currents were amplified by an EPC-7 amplifier (List Electronic Darmstadt, Germany), filtered at 2 Hz (–3 dB) and acquired at a sample rate of 5 kHz on a microcomputer for off-line analysis (pClamp 6, Axon Instruments, Foster City, CA, USA). Cell capacitance of the recorded cell was estimated by on-line electronic correction of capacitive transients. Values of current density were calculated by dividing the whole-cell currents by the cell capacitance. Capsaicin and capsazepine were dissolved in DMSO at a concentration of 10 mM and diluted to the working concentration of 1 μ M for capsaicin and 10 μ M for capsazepine in external solution the same day of the experiment.

Hot plate test

Mice of age 8–12 weeks (≈ 30 g) were used for the study. The animals were positioned in the experimental room 1 h before the test. DD04107 (kindly provided by BCN Peptides) was diluted in 0.9% saline and was administered subcutaneously at the doses of 3 mg/kg ($n_{WT} = 14$; $n_{KO} = 14$). For the control groups of experiments, 100 μ l of 0.9% saline was administered subcutaneously ($n_{WT} = 15$; $n_{KO} = 15$).

Each mouse was placed into a transparent beaker made of Plexiglas of 60 cm and a diameter of 18 cm to avoid the animals escaping from the plate which temperature was set at $52^{\circ}\text{C} \pm 0.1^{\circ}\text{C}$ by using a thermo-regulated heated plate (Ugo Basile, Varese, Italy). The time (in seconds) between the placement of the animal and the first response: paw licking/fanning or jumping was measured as latency. A 30-s cut-off was used to prevent tissue damage. The measurements started 2 h after the administration of saline/DD04107 and were repeated in intervals of 4, 8, 24, 48, 56, and 168 h.

Data acquisition

Fluorescent images were captured with a Nikon D-Eclipse C1 inverted laser scanning confocal microscope. Images were collected as single focal sections separately for each channel. EZ-C1 3.90 Free Viewer, Image J (NIH), and Adobe Photoshop software were used for image capture and analysis.

Statistical analysis

ImageJ (gel analyser plugin) was used for quantification of Western blots; and GraphPad Prism 5 (GraphPad Prism Software) was used to perform an Fisher's exact test for statistical significance for differences in protein expression and unpaired paired Student's *t*-test one-tailed for electrophysiological results and whole DRGs section evaluation. Two-way repeated-measure ANOVA followed by least significant difference Fisher's post hoc test was performed to analyze behavioral data. Values shown represent mean \pm SEM. A *P*-value of <0.05 (*), $p < 0.01$ (**), and $p < 0.001$ (***)

Results

Altered innervation of α -GalA(-/0) mice dorsal skin

Mutant genes were determined as previously described by Lakomá et al.¹³ We recently reported that the expression of the neuronal marker PGP9.5 showed a significant decreased and scattered pattern of neuronal terminations in the frontal skin paw of α -GalA(-/0) males in

comparison to their WT littermates. This parallels the observation of a decrease in neuronal terminations marked by PGP9.5 in skin biopsies of human patients with small fiber neuropathies.^{14,31} Thus, we next examined the epidermis of dorsal skin of α -GalA(-/0) individuals compared with WT mice. Since we observed, the disease severity affects more strongly males than females, we focused our study only on males. The immunohistochemistry of floating sagittal sections of mice back skin biopsies revealed a significant decrease in dermal PGP9.5 positive neuronal terminations in α -GalA(-/0) mice (Figure 1(a) white arrows). Notably,

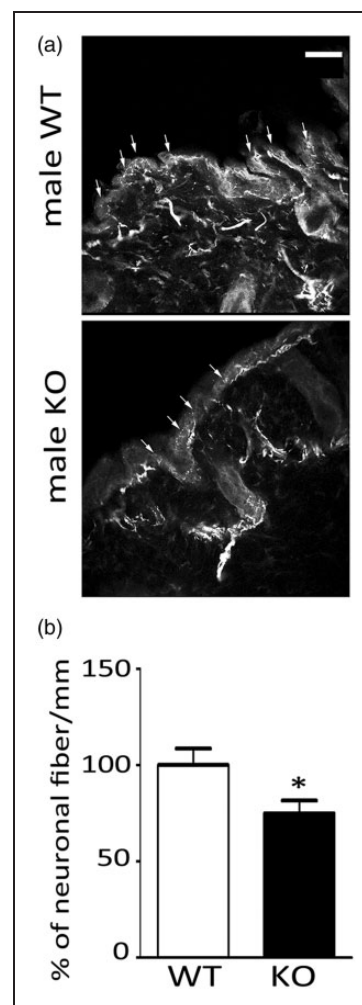


Figure 1. Innervation of α -GalA KO mouse skin biopsy. (a) The immunostaining of 50 μ m floating sagittal sections of mice back skin biopsy revealed a decrease in PGP9.5 positive innervation (white) in α -GalA KO males ($n = 3$) in comparison to their WT controls ($n = 3$). Scale bar represents 100 μ m. (b) Quantitative analysis of neuronal fibers terminations in epidermis of mice back skin biopsy showed significant decrease (about 30%; $p = 0.0179$) in α -GalA KO males in comparison to WT.

density of the epidermal nerve fibers was significantly decreased in α -GalA(-/0) mice compared with WT (30% less PGP 9.5 positive fibers in α -GalA(-/0) (2.44 fibers/mm) in comparison to WT (3.26 fibers/mm); Figure 1, $p=0.02$, $n=3$ animals for WT and GalA(-/0)). These results substantiate our previous observation in α -GalA(-/0) mice frontal paws¹³ and indicates a general phenotype for peripheral nervous system (PNS) in FD in the animal model that matches that of humans.

Morphological structure and characterization of WT versus KO DRG neurons

To examine the morphology and level of Gb3 expression in WT and α -GalA(-/0) DRG neurons, III beta-tubulin (Tuj-1), Gb3, and NeuN expression were monitored by immunocytochemistry (Figure 2). NeuN was used as a neuron-specific nuclear protein determining the neuronal specificity of neurons in the primary culture isolated from DRGs. The cytoplasm marker of most neuronal cell types Tuj-1 was employed to visualize the neurites length and morphology of neuronal cell body. Interestingly, we observed a high level of expression of Gb3 in α -GalA(-/0) DRGs in comparison to WT

(Figure 2(b) from middle panel). This increased expression corroborates the accumulation of Gb3 in sensory terminals as a hallmark of FD. In addition, α -GalA(-/0) DRG terminals show a significant volume increase compared with WT as evidenced by Tuj-1 labeling of DRG neuronal bodies (Figure 2(c),f) $p=0.0168$, $n=3$ animals).

Increase of TRPV1 protein expression in Fabry mice DRG neurons

We have recently proposed that the higher pain perception in Fabry patients and the in α -Gal A(-/0) mice is primarily due to an altered peripheral expression of ion channels involved in sensory pain transduction such as TRPV1, TRPM8, and Nav1.8, as that detected in peripheral terminals.¹³ Next, we sought to substantiate this tenet in in vitro-cultured DRG neurons isolated from α -GalA(-/0) and WT mice. We evaluated the expression of TRPV1, TRPM8, and Nav1.8 in primary cultures of DRG neurons from α -GalA(-/0) and WT male mice. As illustrated by Figure 3(a) to (d), we observed a higher fluorescent signal of TRPV1 in α -GalA(-/0) than in WT nociceptors. This finding was further

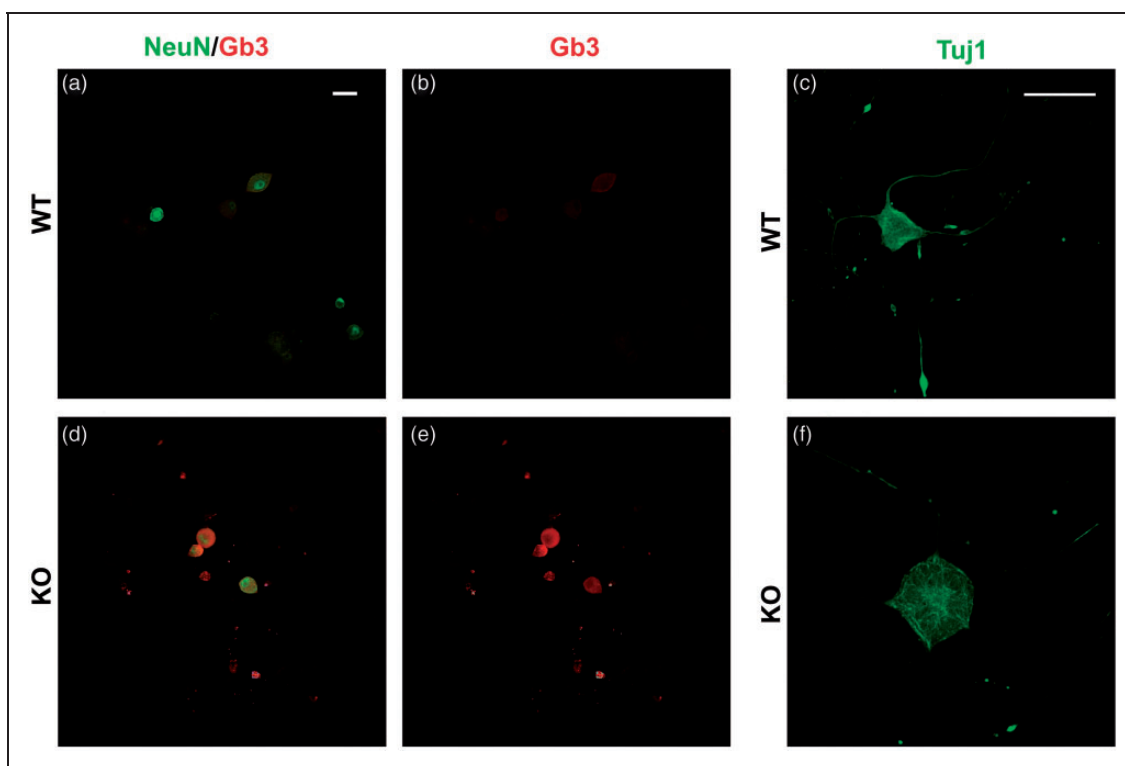


Figure 2. Characterization of DRG neurons in culture from WT (a-b-c) and KO mice (d-e-f). Immunocytochemistry of NeuN positive (green) DRG neurons clearly shows accumulation of globotriaosylceramide (Gb3) (red) in the cells of KO in comparison to WT mice. III beta-tubulin (anti-Tuj1) staining of DRGs (green, right panel) showed significant increase ($p=0.0168$) in the KO DRG neurons ($n=73$) in comparison to WT ($n=72$). Scale bars represent 50 and 25 μ m.

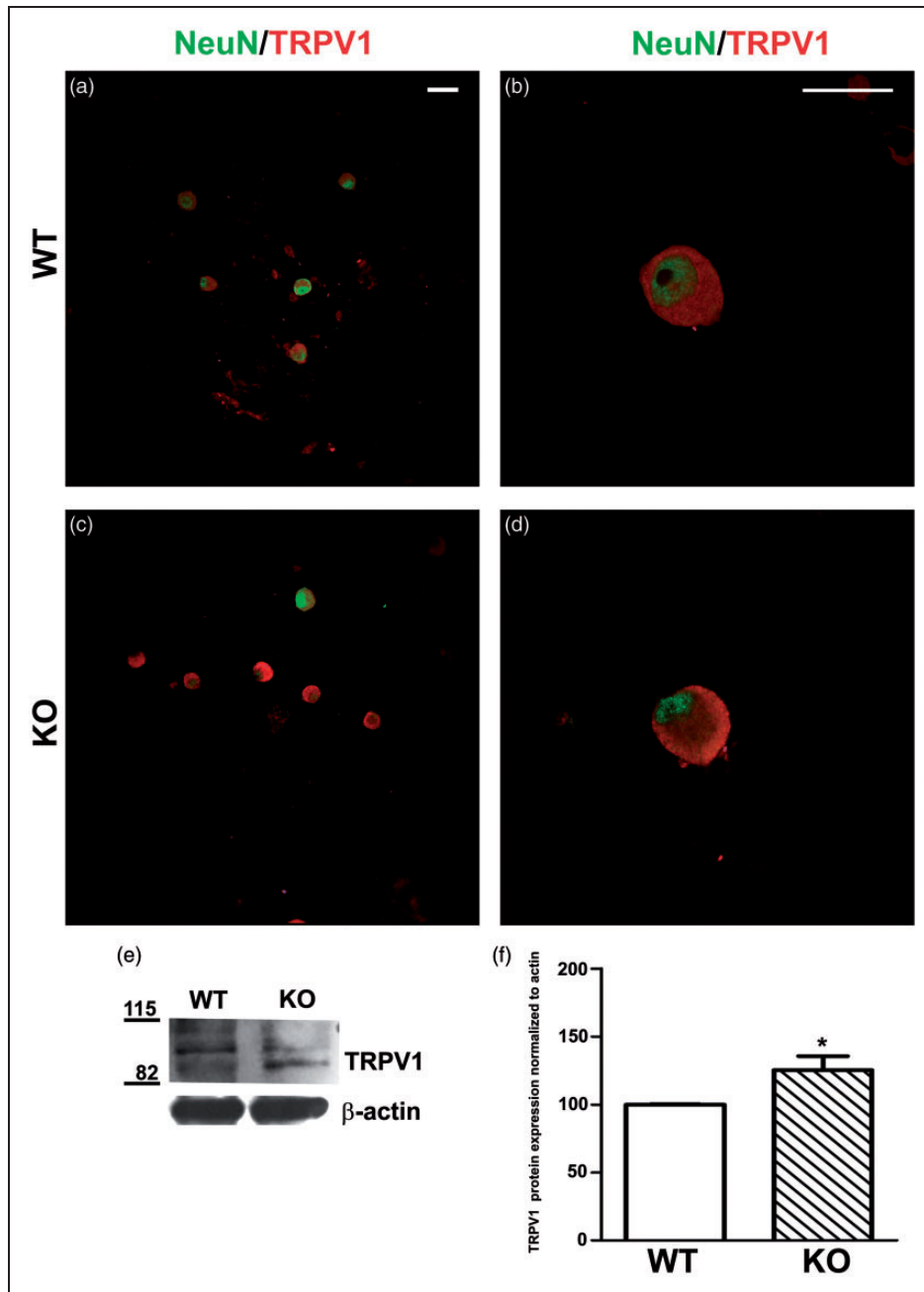


Figure 3. TRPV1 detection in seven days cultured DRG neurons. (a–c) Immunocytochemistry of DRGs from α -GalA KO males ($n = 5$) showed different expression at the protein level of the specific TRPV1 receptor (red) in comparison to their WT controls ($n = 5$). The neuronal nuclear lineage-specific marker NeuN is shown in green. (b–d) High magnification of DRG neurons double stained for TRPV1 (red) and NeuN (green). (e) The Western blot analysis of TRPV1 expression $\sim 92/110$ – 113 kDa. (f) The quantitative analysis of three independent experiments of TRPV1 expression immune-blot in the whole protein extract from DRGs cultures pooled from five males for each genotype showed the 25% increase in protein expression of TRPV1 in case of α -GalA KO males when compared with WT ($p = 0.030$). The scale bars represent 50 and 25 μ m.

confirmed by quantitative Western Blot analysis. In fact, protein expression analysis revealed a 1.25-fold increase of TRPV1 protein expression in the total DRG protein extraction from α -GalA($-/0$) mice compared with WT (Figure 3(e), (f) $p = 0.03$, $n = 5$ animals). In contrast, TRPM8 levels were not altered in the α -GalA($-/0$)

nociceptors (Figure 4, $p = 0.3$, $n = 5$). A similar result was obtained for the levels of Nav1.8 (Figure 5, $p = 0.4$, $n = 5$). These results corroborate that the thermal hyperalgesia previously detected in in vivo Fabry murine model¹³ is mainly due to an increased protein expression of TRPV1 in DRG nociceptors.

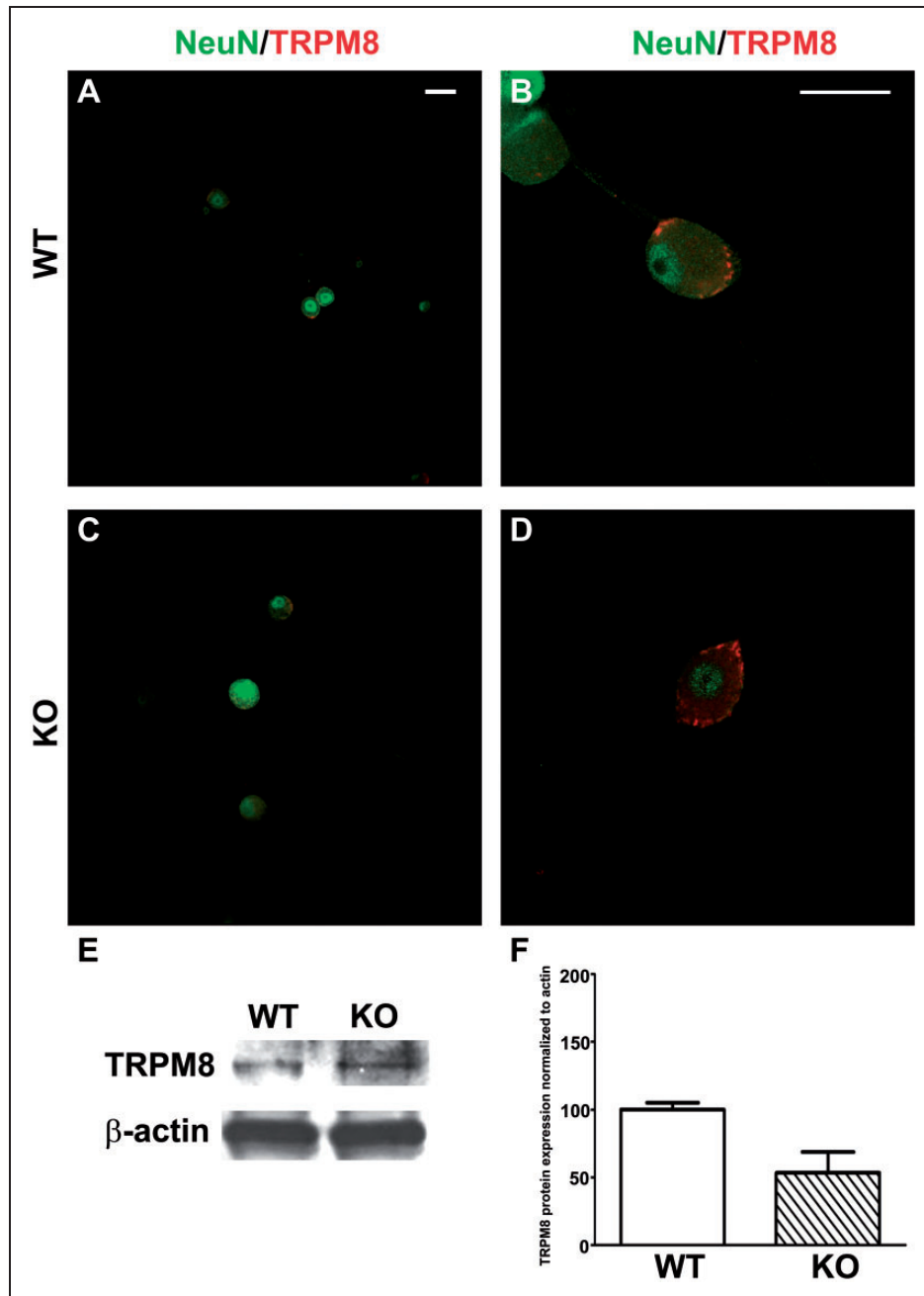


Figure 4. TRPM8 detection in seven days cultured DRG neurons. (a–c) Immunocytochemistry of DRGs from α -GalA KO males ($n = 5$) showed similar expression at the protein level of the specific TRPM8 receptor (red) in comparison to their WT controls ($n = 5$). The neuronal nuclear lineage-specific marker NeuN is shown in green. (b–d) High magnification of DRG neurons double stained for TRPM8 (red) and NeuN (green). (e) The Western blot analysis of TRPM8 expression (~ 127 kDa) revealed no differences in the protein expression in case of α -GalA KO males ($n = 5$) when compared with WT ($n = 5$). (f) The quantitative analysis of two independent experiments of TRPM8 expression immuno-blot in the whole protein extract from DRGs cultures pooled from 2–3 males for each genotype clearly showed no differences in protein expression of TRPM8 in case of α -GalA KO males when compared with WT. The scale bars represent 50 and 25 μ m.

TRPV1 receptor immunostaining in α -GalA(–/0) DRG sections

We next performed immunohistochemical staining on mice DRG cryosections from α -GalA(–/0) mice, in

order to check receptor distribution in sensory fibers and prove whether TRPV1 was overexpressed not only in the in vitro condition. In Figure 6, representative hematoxylin/eosin staining for anatomical demonstration of DRGs and immunofluorescence images are

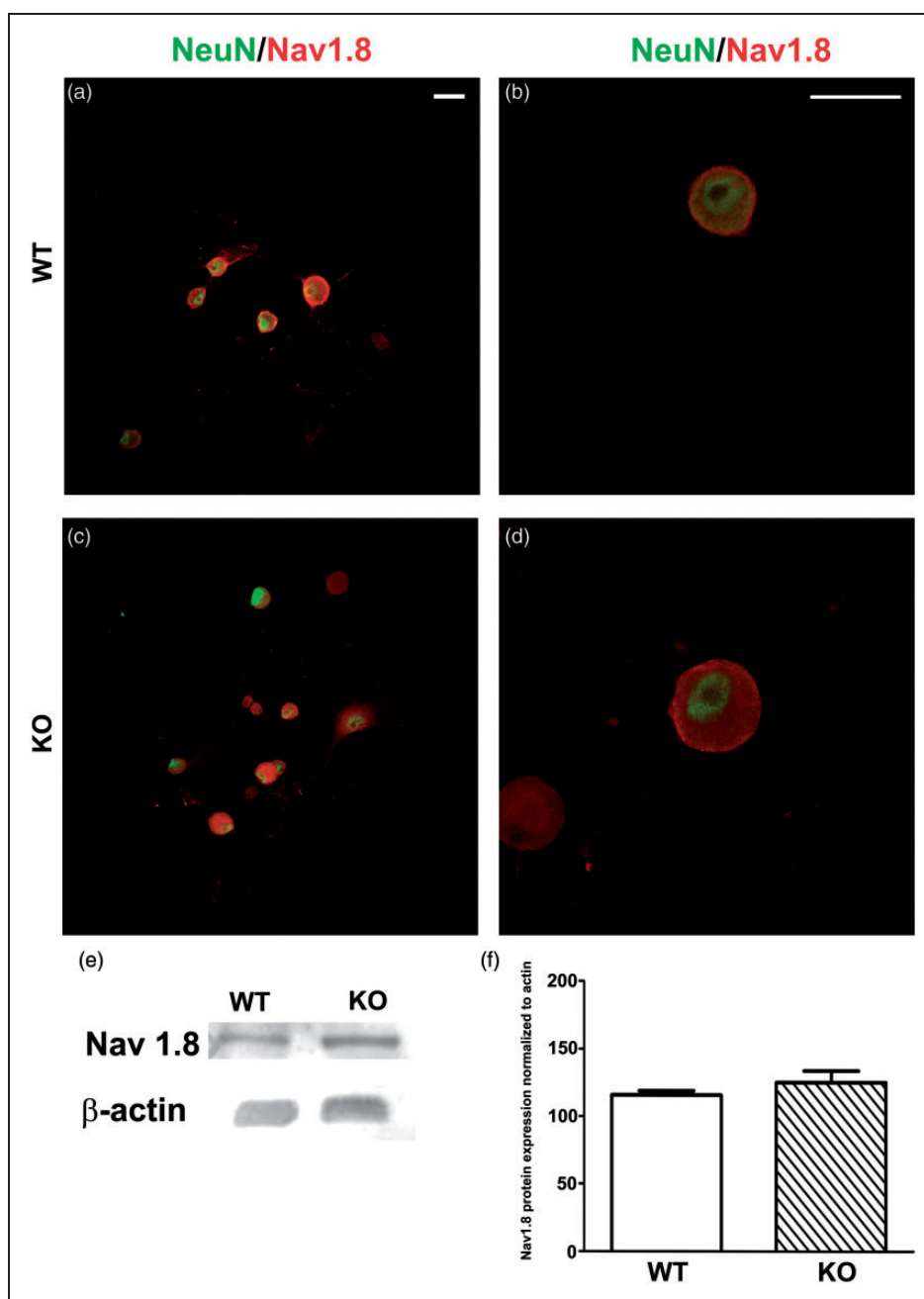


Figure 5. Nav1.8 detection in seven days cultured DRG neurons. (a–c) Immunocytochemistry of DRG neurons from α -GalA KO males ($n = 5$) showed slightly different expression at the protein level of the specific Nav1.8 receptor (red) in comparison to their WT controls ($n = 5$). The neuronal nuclear lineage-specific marker NeuN shown in green. (b–d) High magnification of DRG neurons double stained for Nav1.8 (red) and NeuN (green). (e) The Western blot analysis of Nav1.8 expression (~ 220 kDa) revealed no difference in protein expression in case of α -GalA KO males ($n = 5$) when compared with WT ($n = 5$). (f) The quantitative analysis of two independent experiments of Nav1.8 expression immune-blot in the whole protein extract from DRGs cultures pooled from three males for each genotype clearly showed no differences in protein expression of Nav1.8 in case of α -GalA KO males when compared with WT. The scale bars represent 50 and 25 μ m.

reported. The morphological structure of the α -GalA(–/0) mice model DRGs and their WT littermates, stained with hematoxylin and eosin staining, showed a fully developed DRG neurons system without histological alterations in both genotypes (Figure 6(a) and (d)).

Conversely, the Gb3 positive staining was observed exclusively in the sections of α -GalA(–/0) DRG (Figure 6(b) and (e)). In parallel, the α -GalA(–/0) mice neurons exhibits a more pronounced positive staining for TRPV1 compared with controls (Figure 6(c) and (f)).

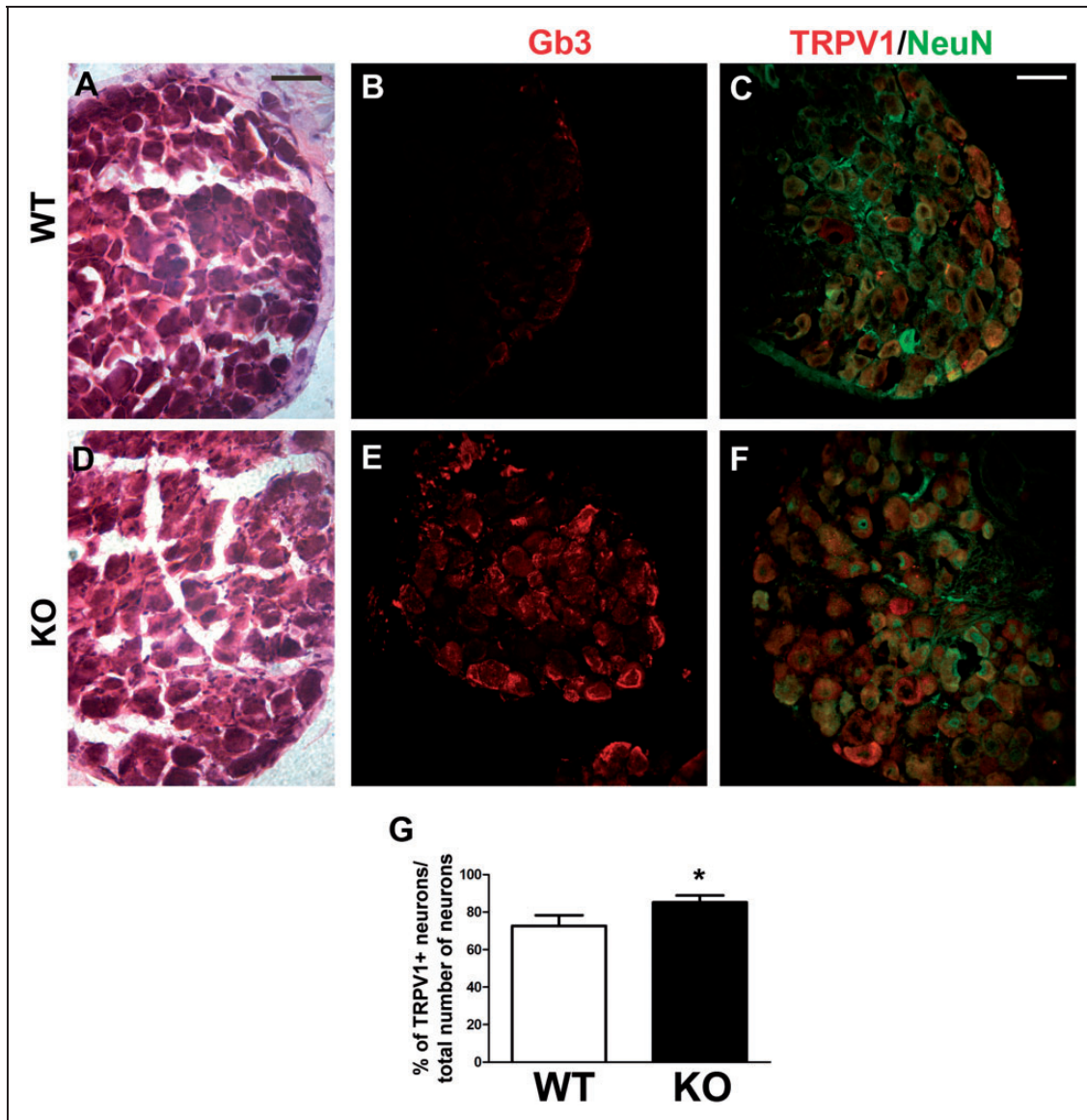


Figure 6. TRPV1 and Gb3 expression in whole DRG. Cryostat sections (20 μ m) of DRG from α -GalA(-/0) and WT, were stained with hematoxylin/eosin (a, d) and (10 μ m) immunostained with antibodies for Gb3, TRPV1, and NeuN (b-f). The quantitative analysis of two independent TRPV1/NeuN immunostainings in whole DRG revealed significant increase ($p = 0.0306$) in TRPV1 expressing neuronal population of α -GalA(-/0) mice in comparison to their WT controls (g). $n = 27$ for both WT and KO represents the number of randomly chosen images for final evaluation; for each genotype were used three males of eight weeks of age. Representative immunofluorescence images are reported. The scale bars represent 100 μ m.

Taking together, these results indicate that TRPV1 is again overexpressed in the cryosections of whole trigeminal ganglia isolated DRG neurons from α -GalA(-/0) mice compared with control littermates (Figure 6(g)).

Functional expression of TRPV1 receptor in α -GalA(-/0) DRG neurons

A question that emerges is whether the augmented protein expression of TRPV1 in nociceptors was paralleled by an increased activity as higher protein expression does

not necessarily results in augmented TRPV1 responses due to potential channel clustering.^{32,33} Thus, we next evaluated capsaicin-activated currents by patch-clamp in whole cell configuration. It should be noted that we frequently observed in DRG neurons of α -GalA(-/0) mice that the cell membrane was extremely sticky and easily perforated by the patch-electrode giving rise to low-resistance seals. This particular characteristic was even more noticeable in the plasma membrane of neurons isolated from older animals (the time window of animals used for DRG isolation was from 8 to 12

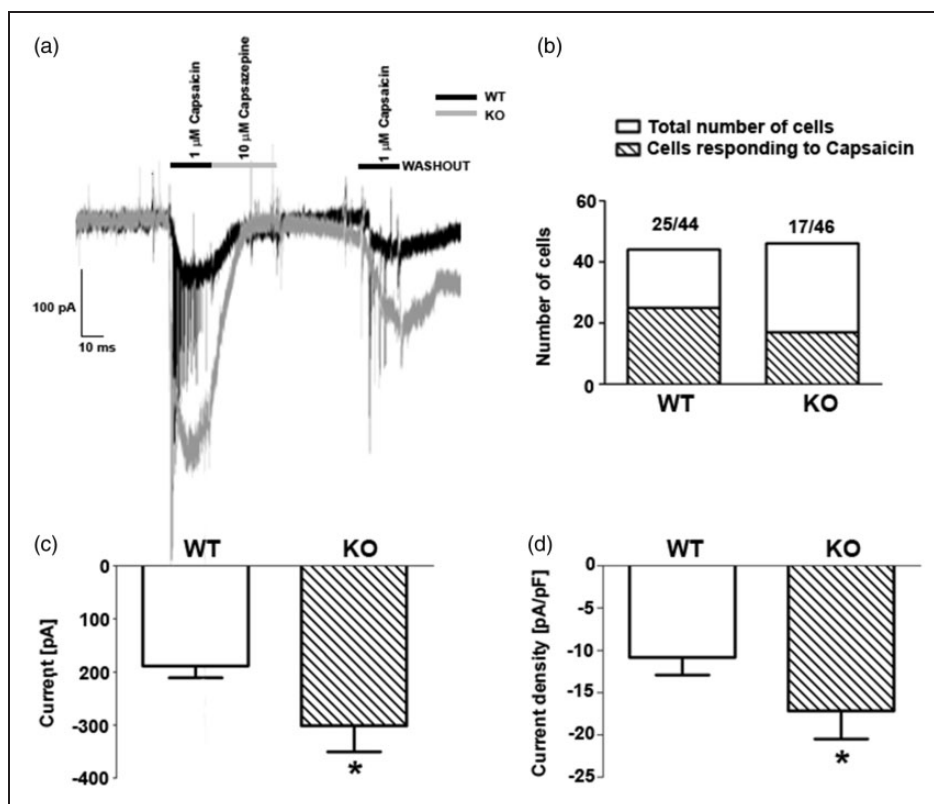


Figure 7. Capsaicin evoked ionic currents from DRG neurons in culture. (a) Representative currents activated by 1 μM capsaicin and blocked by 10 μM capsazepine in $\alpha\text{-GalA}(-/0)$ and control mice. Sensory neurons were held at -60 mV. The amplitude of capsaicin-evoked inward current was greatly increased in a small-diameter dorsal root ganglion (DRG) neuron of $\alpha\text{-GalA}(-/0)$ compared with capsaicin-induced inward cationic current in a control small DRG sensory neuron. Compared with capsaicin-induced inward cationic current in a control small DRG sensory neuron, the amplitude of capsaicin-evoked inward current was greatly increased in a small-diameter DRG neuron from $\alpha\text{-GalA}(-/0)$ (b) Percentage of capsaicin responding cells—the percentage of small diameter DRG neurons responding to 1 μM capsaicin stimuli was lower in $\alpha\text{-GalA}(-/0)$ (35%) in comparison to its WT control (60%). (c) Quantitative representation of TRPV1 currents recorded at -60 mV. Values are given as means \pm SE; $n = 8$ for WT and $n = 5$ for KO cells. * $p < 0.0184$. (d) Quantitative assessment of TRPV1 currents density by normalization of peak current recorded at -60 mV to the capacitance of each cell. Values are given as means \pm SE; $n = 8$ for WT and $n = 5$ for KO cells. * $p < 0.05$.

weeks). Most likely, due to this fact, we patched a lower number of nociceptors of $\alpha\text{-GalA}(-/0)$ than from WT mice. Figure 7(a) depicts that small diameter DRG neurons responded to 1 μM capsaicin application by activating an inward cationic current of ≥ 150 pA in WT DRG nociceptors and ≥ 300 pA in KO DRG neurons (Figure 7(a), (c)). This current was fully blocked by 10 μM capsazepine. A quantitative assessment of the TRPV1 activity measuring the capsaicin current density shows that $\alpha\text{-GalA}(-/0)$ nociceptors had a mean -17.15 pA/pF at a holding potential of -60 mV (Figure 7(d)), while WT nociceptors exhibited -10.84 pA/pF, demonstrating a statistical enhancement of the TRPV1 current in the dissociated nociceptive DRG neurons in vitro. Intriguingly, the percentage of nociceptors responding to capsaicin was significantly lower in $\alpha\text{-GalA}(-/0)$ nociceptor primary cultures (Figure S1(a), 35% of $\alpha\text{-GalA}(-/0)$ and 60% for WT DRG neurons responded to capsaicin). It is worth to

mention that during the experimental window of 72 h after cellular plating, we observed the decrease in the TRPV1 capsaicin-evoked currents with the time of culture. This can lead the hypothetical decrease in sensibility to capsaicin-activated currents in older DRG neurons (Figure S1C, D).

Thermal sensitivity of $\alpha\text{-GalA}(-/0)$ is attenuated by blocking regulated exocytosis

The finding that TRPV1 is highly expressed in nociceptors from $\alpha\text{-GalA}(-/0)$ mice suggest that these mice may exhibit higher thermal sensitivity than WT animals. To evaluate the thermal nociception of the transgenic and WT mice, we measured the latency to the first response in the hot-plate test at $52^\circ\text{C} \pm 0.1^\circ\text{C}$. As depicted in Figure 8(a), $\alpha\text{-GalA}(-/0)$ mice exhibited a ≈ 2 -fold lower latency to the noxious heat stimulus than WT mice, indicating an augmented thermal sensitivity of

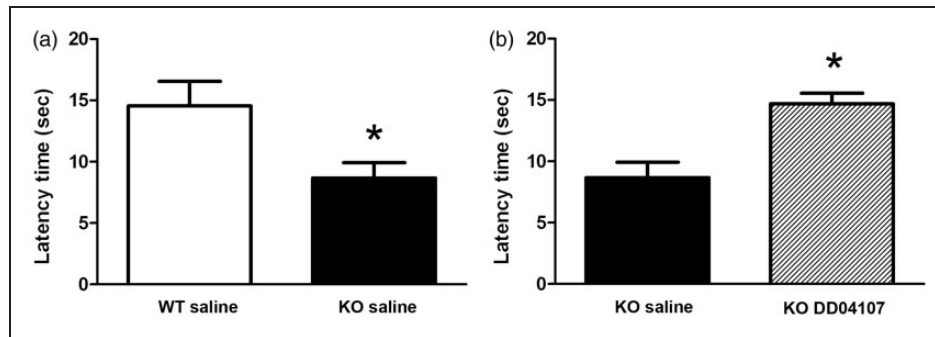


Figure 8. Decrease in thermal sensitivity. (a) The statistically significant reduction in latency time of male KO group 2 h after the administration of saline demonstrates higher acute sensitivity to noxious hot thermal stimulation than in WT male group ($p = 0.01$, $n = 14$ animals for WT, $n = 14$ animals for KO). (b) The same interval of 2 h after the subcutaneous administration of 3 mg/kg DD04107 peptide showed significantly reduced thermal sensitivity generated in the α -GalA(-/0) mouse model of FD ($n = 15$) by hot-plate stimulus of $52^\circ\text{C} \pm 0.1^\circ\text{C}$ when compared with α -GalA(-/0) KO mice injected with saline ($n = 14$) ($p = 0.02$). Two-way ANOVA for Treatment effect $F(1, 54) = 1.32$, $p = 0.25$; Genotype effect: $F(1, 54) = 4.01$, $p = 0.05$; Genotype effect \times Treatment effect $F(1, 54) = 5.02$, $p = 0.02$.

the transgenic mice. This enhanced thermal sensitivity may be due to an increased TRPV1 activity and/or to an enhanced surface expression of the receptor.^{34–36} Indeed, it has been reported that TRPV1 sensitization in nociceptors is in part due to the algescic-induced exocytotic recruitment of this receptor to the neuronal surface of peptidergic nociceptors.^{21,37} Blockade of Ca^{2+} -dependent exocytosis in nociceptors using compound DD04107 prevents the algescic-induced exocytotic recruitment of TRPV1^{21,37} and produces thermal antinociception in models of chronic pain.^{37,38} Thus, we hypothesized that blockade of neuronal exocytosis may modulate the surface expression of TRPV1 in α -GalA(-/0) nociceptors and attenuate the thermal hypersensitivity of the transgenic mice. To address this hypothesis, we evaluated the effect on the thermal nociception of peptide DD04107 (3 mg/kg, s.c.) in α -GalA(-/0) mice (Figure 8(b)). As illustrated, injection of the peptide resulted in a significant reduction of the thermal sensitivity as revealed by the increase of the latency to the heat response up to the level of WT animals. Furthermore, the peptide effect lasted up to 24 h post injection (Figure S2). As reported previously,³⁸ peptide DD04107 did not have a significant effect on the thermal nociception of WT animals (data not shown). These results imply that the augmented thermal nociception of α -GalA(-/0) mice may be attenuated by blocking regulated exocytosis in nociceptors and suggest that the enhanced expression of TRPV1 in α -GalA(-/0) nociceptors may produce an increment in the membrane recruitment of the channel leading to heat hypersensitivity.

Discussion

FD is a rare multisystemic inherited metabolic disease with profound effects on almost all organs.³⁹ FD has a

childhood onset and frequently leads to early mortality of untreated patients.⁴⁰ Neuropathic pain and somatosensory disturbances are often the first representative symptoms in FD and can be episodic, with agonizing burning pain in the hands and feet, or chronic, with burning or shooting pain, or dysesthesias.⁴¹ The pathophysiology of the altered sensory neurons function in FD remains poorly understood. The manifestations at the neurological level occur in both the PNS and CNS. The important consequences of Gb3 accumulation were assigned to a potential mechanism of cerebral ischemia in FD patients which results from Gb3 storage in the vascular epithelium. Gb3 accumulation in neurons of CNS is predominantly involved in the cerebrovascular events⁴² characterized by cerebral vasculopathy, various anatomical abnormalities (e.g., small and large vessels), impairment of endothelial function,^{43,44} and cerebral blood flow dysregulation;⁴⁵ in early age at onset and abnormal brain magnetic resonance imagings. Early treatment of FD patients with enzyme replacement therapy (ERT) is the key therapeutic goal to avoid multiple organ damage.¹⁰ Interestingly, the evidence of the ERT beneficial effects is reported in the improvement of Gb3 reduction in organ and tissues.⁴⁶ Nevertheless, minimum of six months treatment is required to reveal the positive effect of ERT on neuropathic pain.^{47,48}

Recently, the characterization of a FD mouse model^{49,50} opened the possibility to interrogate the functional and structural involvement of PNS components in the mechanism contributing to pain in FD patients. Rodrigues et al.⁵¹ published a detailed histological analysis of cytoarchitecture of Fabry mice sciatic nerves. There was also observed the lipid accumulation in DRG of Fabry patients, even its effect on sensory neurons was not studied.^{12,52} Furthermore, the group of Choi et al.^{16,20,53} has concentrated their scientific interest

into the effect on FD-associated lipid Lyso-Gb3 (deacetylated form of Gb3) in DRG neurons of adult mice and cellular fibroblast line. The nature and temporal effects of the Gb3 substrate accumulation on tissue histology in Fabry mice was recently characterized by Bangari et al.⁵⁴ It is important to highlight that Shen and coworkers recently published a detailed study employing a new derivative of alpha-Gal (Moss alpha-Gal; which is identical to the native human alpha-Gal) in mice FD model, proposing this enzyme as a future possible agent for ERT of Fabry patients.⁵⁵ In this context, it would be an interesting idea to unveil the ERT effect on neuropathic pain in FD mouse model.

The plasma circulation of Lyso-Gb3 and the concomitant lysosomal accumulation of Gb3 in sensory neurons has been proposed to lead to pain in FD.⁵⁶ Moreover, it has been demonstrated that the intraplantar injection of Lyso-Gb3 in healthy mice developed mechanical allodynia through sensitizing of DRG neurons. In parallel, the effect of Lyso-Gb3 incubation on mice sensory neurons led to a significant enhancement of voltage-gated calcium currents and intracellular Ca^{2+} in capsaicin positive sensory neurons.¹⁶ In the present study, we hypothesized that during chronic inflammatory or neuropathic pain, upregulated TRPV1 channels induce hyperactivity of DRG nociceptive neurons and thermal sensitivity by directly enhancing the channel function. According to our previous findings, the α -GalA(-/0) male mouse is an appropriate disease model to study the peripheral small fiber neuropathy exhibited by FD patients and to provide molecular evidence for the hyperexcitability of small nociceptors in FD.^{13,14} In parallel, the dysfunctions of ion channels widely distributed in human A δ and C-fibers has been proposed to be involved in pain transmission and sensation in small fiber neuropathies.^{57,58}

The main goal of the present study was to examine and characterize the DRG neurons of FD mice model in comparison to WT group in order to provide evidence consistent with an overexpression of ion channels that directly link the Gb3 accumulation in peripheral sensory neurons and pain in FD. In this context, our previous results have demonstrated an elevated expression of Nav1.8 and TRPV1, but not TRPM8, in the epidermis of α -GalA(-/0) males glabrous skin of frontal paws in comparison to control WT group.¹³ In addition, the expression of the neuronal marker PGP9.5 specific for neuronal terminations in the skin showed a significantly decreased and scattered pattern of neuronal terminations in α -GalA(-/0) males as was previously observed in human skin.^{13,31,59}

To support the observation that pain sensitivity in α -GalA(-/0) males was due to ion channels alterations in the expression, distribution, and function, we first employed immunohistochemistry for detection of these channels protein previously described in glabrous skin of

mice frontal paws.¹³ The immunostaining and protein quantification using the TRPV1 antibody, in vitro cell cultures of DRG neurons and in cryosections of whole DRGs, indicate an increased expression of receptor directly in the DRG of α -GalA(-/0) males compared with DRG of α -GalA(+/0) males. On the other hand, no significant differences in TRPM8 and Nav1.8 expression were observed in α -GalA(-/0) mice compared with controls. Our experimental evidences support the hypothesis that the overexpression of TRPV1 channels observed in the Fabry model generates alterations in action potential generation and propagation resulting in producing pain. The functional evaluation of TRPV1 in the native neuronal systems revealed a capsaicin activation more pronounced in terms of total current and current density of the α -GalA(-/0) DRG neurons compared with WT DRG neurons. A consequence of the higher TRPV1 activity in α -GalA(-/0) sensory neurons is that these mice exhibit a higher thermal sensitivity than WT littermates, as evidenced from the shorter latency times in the hot plate test. Here, we hypothesized that the increased thermal nociception in α -GalA(-/0) mice may result, at least in part, from an augmented expression of TRPV1 in the DRGs peripheral terminals.¹³ Noteworthy, blocking of neuronal exocytosis with compound DD04107, which inhibits the exocytotic recruitment of TRPV1 channels to the neuronal surface in peptidergic nociceptors^{21,37,38} resulted in a significant attenuation of thermal sensitivity in α -GalA(-/0) mice, consistent with the tenet that the enhanced thermal nociception of the α -GalA(-/0) mice may be due to an increased membrane recruitment of TRPV1 in nociceptors. Although the susceptibility of the thermal nociception of α -GalA(-/0) mice to peptide DD04107 suggests that the thermal hypersensitivity of α -GalA(-/0) mice may be due to an augmented surface expression of TRPV1 in α -GalA(-/0) nociceptors, additional experiments are needed to demonstrate that an enhanced membrane translocation of TRPV1 pivotally contributes to the pain phenotype in FD patients. Nonetheless, it is worth noting that the in vivo anti-nociceptive activity of peptide DD04107 in α -GalA(-/0) mice implies a potential novel therapeutic strategy to reduce the pain sensitivity in FD patients.

Author Contributions

JL managed the maintaining of the mice colony, designed, and performed all the molecular and immunostaining experiments and their analyses, wrote the paper. RR performed the behavioral experiments and revised critically the manuscript; AF revised critically the manuscript and wrote the paper; VD and RL, revised critically the manuscript and contributed reagents; MC conceived, designed and supervised the project, wrote the paper. All authors read and approved the final manuscript.

Declaration of Conflicting Interests

The author(s) declared no potential conflicts of interest with respect to the research, authorship, and/or publication of this article.

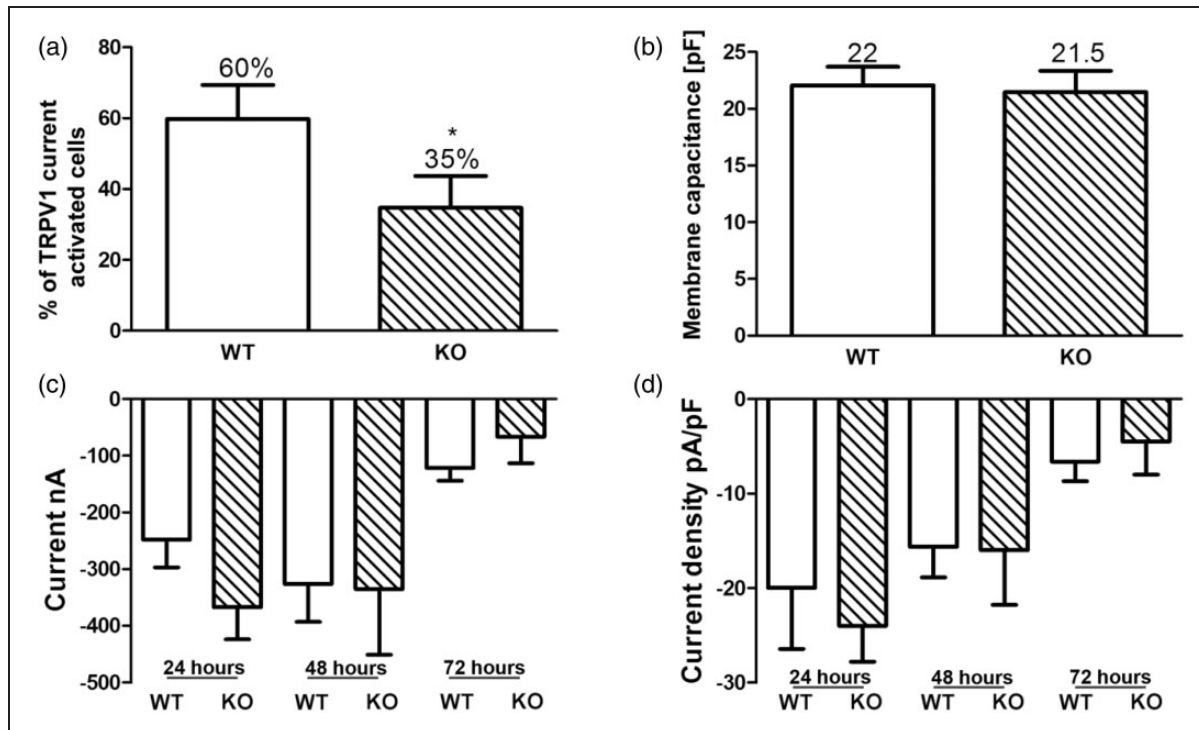
Funding

The author(s) disclosed receipt of the following financial support for the research, authorship, and/or publication of this article: We are grateful to Alessia Minardi, Alex Incensi, Maria Pia Culcasi, and Prof. Stefano Ferroni. We thank BCN Peptides (Barcelona) for kindly providing DD04107. This work was supported by the contract grant sponsor Ministero della Salute, Bando Progetti di Ricerca Finalizzata IRCCS—Istituto delle Scienze Neurologiche di Bologna, Italy, (contract grant number: 2010 RF-2010-2313899) grant to M.C., R.L., V.D., and R.R.; and a Grant from the MINECO/FEDER, EU (SAF2015-66275-C2-1-R), and from the Generalitat Valenciana, Spain (PROMETEO/2014/011).

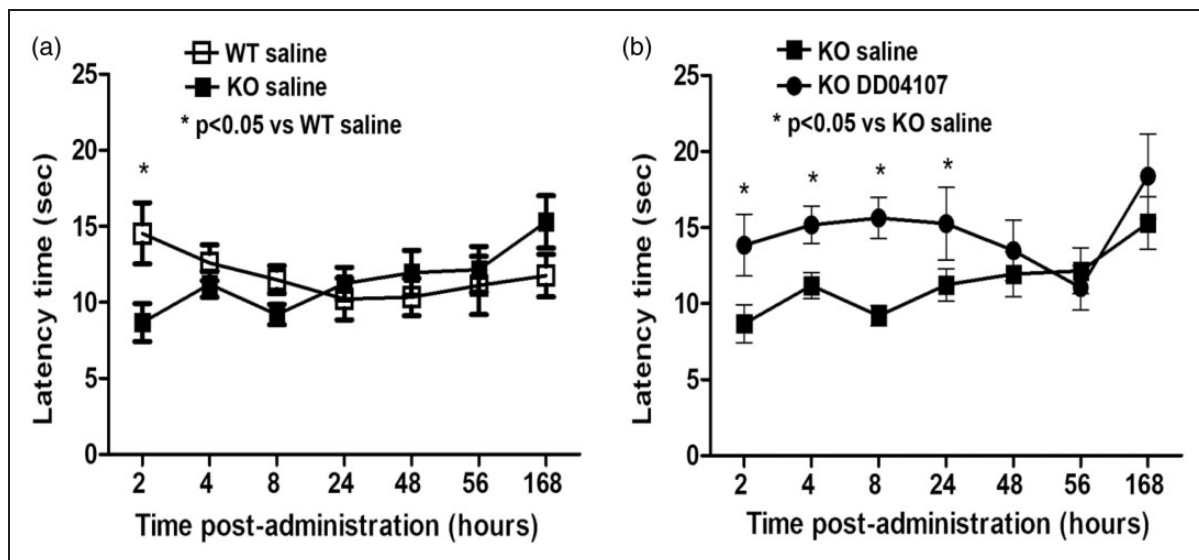
References

- Brady RO. Enzymatic abnormalities in diseases of sphingolipid metabolism. *Clin Chem* 1967; 13: 565–577.
- Germain DP. Fabry disease. *Orphanet J Rare Dis* 2010; 5: 30.
- Magg B, Riegler C, Wiedmann S, et al. Self-administered version of the Fabry-associated pain questionnaire for adult patients. *Orphanet J Rare Dis* 2015; 10: 113.
- Gibas AL, Klatt R, Johnson J, et al. A survey of the pain experienced by males and females with Fabry disease. *Pain Res Manag* 2006; 11: 185–192.
- Schaefer RM, Tylki-Szymanska A and Hilz MJ. Enzyme replacement therapy for Fabry disease: a systematic review of available evidence. *Drugs* 2009; 69: 2179–2205.
- Tarabuso AL. Fabry disease. *Skinmed* 2011; 9: 173–177.
- Biegstraaten M, Binder A, Maag R, et al. The relation between small nerve fibre function, age, disease severity and pain in Fabry disease. *Eur J Pain* 2011; 15: 822–829.
- Liguori R, Di SV, Bugiardini E, et al. Small fiber neuropathy in female patients with Fabry disease. *Muscle Nerve* 2010; 41: 409–412.
- Uceyler N and Sommer C. [Fibromyalgia syndrome: a disease of the small nerve fibers?]. *Z Rheumatol* 2015; 74: 490–495.
- Burlina AP, Sims KB, Politei JM, et al. Early diagnosis of peripheral nervous system involvement in Fabry disease and treatment of neuropathic pain: the report of an expert panel. *BMC Neurol* 2011; 11: 61.
- Kaye EM, Kolodny EH, Logigian EL, et al. Nervous system involvement in Fabry's disease: clinicopathological and biochemical correlation. *Ann Neurol* 1988; 23: 505–509.
- Gadoth N and Sandbank U. Involvement of dorsal root ganglia in Fabry's disease. *J Med Genet* 1983; 20: 309–312.
- Lakoma J, Rimondini R, Donadio V, et al. Pain related channels are differentially expressed in neuronal and non-neuronal cells of glabrous skin of Fabry knockout male mice. *PLoS One* 2014; 9: e108641.
- Lakoma J, Donadio V, Liguori R, et al. Characterization of human dermal fibroblasts in Fabry disease. *J Cell Physiol* 2016; 231: 192–203.
- Choi S, Kim JA, Na HY, et al. Globotriaosylceramide induces lysosomal degradation of endothelial KCa3.1 in Fabry disease. *Arterioscler Thromb Vasc Biol* 2014; 34: 81–89.
- Choi L, Vernon J, Kopach O, et al. The Fabry disease-associated lipid Lyso-Gb3 enhances voltage-gated calcium currents in sensory neurons and causes pain. *Neurosci Lett* 2015; 594: 163–168.
- Habib AM and Cox JJ. Pain in Fabry disease: plasma lipids sensitise nociceptors. *Neurosci Lett* 2015; 594: 161–162.
- Geevasinga N, Tchan M, Sillence D, et al. Upregulation of inward rectifying currents and Fabry disease neuropathy. *J Peripher Nerv Syst* 2012; 17: 399–406.
- Schiffmann R and Scott LJ. Pathophysiology and assessment of neuropathic pain in Fabry disease. *Acta Paediatr Suppl* 2002; 91: 48–52.
- Choi JY, Shin MY, Suh SH, et al. Lyso-globotriaosylceramide downregulates KCa3.1 channel expression to inhibit collagen synthesis in fibroblasts. *Biochem Biophys Res Commun* 2015; 468: 883–888.
- Devesa I, Ferrandiz-Huertas C, Mathivanan S, et al. alphaCGRP is essential for algescic exocytotic mobilization of TRPV1 channels in peptidergic nociceptors. *Proc Natl Acad Sci USA* 2014; 111: 18345–18350.
- Abrahamsen B, Zhao J, Asante CO, et al. The cell and molecular basis of mechanical, cold, and inflammatory pain. *Science* 2008; 321: 702–705.
- Quartu M, Carozzi VA, Dorsey SG, et al. Bortezomib treatment produces nocifensive behavior and changes in the expression of TRPV1, CGRP, and substance P in the rat DRG, spinal cord, and sciatic nerve. *Biomed Res Int* 2014; 2014: 180428.
- Czifra G, Varga A, Nyeste K, et al. Increased expressions of cannabinoid receptor-1 and transient receptor potential vanilloid-1 in human prostate carcinoma. *J Cancer Res Clin Oncol* 2009; 135: 507–514.
- Marincsak R, Toth BI, Czifra G, et al. Increased expression of TRPV1 in squamous cell carcinoma of the human tongue. *Oral Dis* 2009; 15: 328–335.
- Selvarajah M, Nicholls K, Hewitson TD, et al. Targeted urine microscopy in Anderson-Fabry disease: a cheap, sensitive and specific diagnostic technique. *Nephrol Dial Transplant* 2011; 26: 3195–3202.
- Iwagaki N, Ganley RP, Dickie AC, et al. A combined electrophysiological and morphological study of neuropeptide Y-expressing inhibitory interneurons in the spinal dorsal horn of the mouse. *Pain* 2016; 157: 598–612.
- Lakoma J, Garcia-Alonso L and Luque JM. Reelin sets the pace of neocortical neurogenesis. *Development* 2011; 138: 5223–5234.
- Giannoccaro MP, Donadio V, Gomis PC, et al. Somatic and autonomic small fiber neuropathy induced by bortezomib therapy: an immunofluorescence study. *Neurol Sci* 2011; 32: 361–363.
- Hamill OP, Marty A, Neher E, et al. Improved patch-clamp techniques for high-resolution current recording

- from cells and cell-free membrane patches. *Pflugers Arch* 1981; 391: 85–100.
31. Donadio V, Incensi A, Giannoccaro MP, et al. Peripheral autonomic neuropathy: diagnostic contribution of skin biopsy. *J Neuropathol Exp Neurol* 2012; 71: 1000–1008.
 32. Ciardo MG, Andres-Borderia A, Cuesta N, et al. Whirlin increases TRPV1 channel expression and cellular stability. *Biochim Biophys Acta* 2016; 1863: 115–127.
 33. Liu M, Willmott NJ, Michael GJ, et al. Differential pH and capsaicin responses of Griffonia simplicifolia IB4 (IB4)-positive and IB4-negative small sensory neurons. *Neuroscience* 2004; 127: 659–672.
 34. Zhang X, Huang J and McNaughton PA. NGF rapidly increases membrane expression of TRPV1 heat-gated ion channels. *EMBO J* 2005; 24: 4211–4223.
 35. Van Buren JJ, Bhat S, Rotello R, et al. Sensitization and translocation of TRPV1 by insulin and IGF-I. *Mol Pain* 2005; 1: 17.
 36. Morenilla-Palao C, Planells-Cases R, Garcia-Sanz N, et al. Regulated exocytosis contributes to protein kinase C potentiation of vanilloid receptor activity. *J Biol Chem* 2004; 279: 25665–25672.
 37. Camprubi-Robles M, Planells-Cases R and Ferrer-Montiel A. Differential contribution of SNARE-dependent exocytosis to inflammatory potentiation of TRPV1 in nociceptors. *FASEB J* 2009; 23: 3722–3733.
 38. Ponsati B, Carreno C, Curto-Reyes V, et al. An inhibitor of neuronal exocytosis (DD04107) displays long-lasting in vivo activity against chronic inflammatory and neuropathic pain. *J Pharmacol Exp Ther* 2012; 341: 634–645.
 39. Pensabene L, Sestito S, Nicoletti A, et al. Gastrointestinal symptoms of patients with Fabry Disease. *Gastroenterol Res Pract* 2016; 2016: 9712831.
 40. El-Abassi R, Singhal D and England JD. Fabry's disease. *J Neurol Sci* 2014; 344: 5–19.
 41. Marchettini P, Lacerenza M, Mauri E, et al. Painful peripheral neuropathies. *Curr Neuroparmacol* 2006; 4: 175–181.
 42. Buechner S, Moretti M, Burlina AP, et al. Central nervous system involvement in Anderson-Fabry disease: a clinical and MRI retrospective study. *J Neurol Neurosurg Psychiatry* 2008; 79: 1249–1254.
 43. Puccio D, Coppola G, Corrado E, et al. Non invasive evaluation of endothelial function in patients with Anderson-Fabry disease. *Int Angiol* 2005; 24: 295–299.
 44. Altarescu G, Moore DF and Schiffmann R. Effect of genetic modifiers on cerebral lesions in Fabry disease. *Neurology* 2005; 64: 2148–2150.
 45. Kornreich R, Bishop DF and Desnick RJ. Alpha-galactosidase A gene rearrangements causing Fabry disease. Identification of short direct repeats at breakpoints in an Alu-rich gene. *J Biol Chem* 1990; 265: 9319–9326.
 46. Wilcox WR, Banikazemi M, Guffon N, et al. Long-term safety and efficacy of enzyme replacement therapy for Fabry disease. *Am J Hum Genet* 2004; 75: 65–74.
 47. Schiffmann R, Warnock DG, Banikazemi M, et al. Fabry disease: progression of nephropathy, and prevalence of cardiac and cerebrovascular events before enzyme replacement therapy. *Nephrol Dial Transplant* 2009; 24: 2102–2111.
 48. Schiffmann R, Hauer P, Freeman B, et al. Enzyme replacement therapy and intraepidermal innervation density in Fabry disease. *Muscle Nerve* 2006; 34: 53–56.
 49. Ohshima T, Murray GJ, Swaim WD, et al. Alpha-Galactosidase A deficient mice: a model of Fabry disease. *Proc Natl Acad Sci USA* 1997; 94: 2540–2544.
 50. Ohshima T, Murray GJ, Nagle JW, et al. Structural organization and expression of the mouse gene encoding alpha-galactosidase A. *Gene* 1995; 166: 277–280.
 51. Rodrigues LG, Ferraz MJ, Rodrigues D, et al. Neurophysiological, behavioral and morphological abnormalities in the Fabry knockout mice. *Neurobiol Dis* 2009; 33: 48–56.
 52. MacDermot J and MacDermot KD. Neuropathic pain in Anderson-Fabry disease: pathology and therapeutic options. *Eur J Pharmacol* 2001; 429: 121–125.
 53. Choi JY and Park S. Role of protein kinase A and class II phosphatidylinositol 3-kinase C2beta in the downregulation of KCa3.1 channel synthesis and membrane surface expression by lyso-globotriaosylceramide. *Biochem Biophys Res Commun* 2016; 470: 907–912.
 54. Bangari DS, Ashe KM, Desnick RJ, et al. alpha-Galactosidase A knockout mice: progressive organ pathology resembles the type 2 later-onset phenotype of Fabry disease. *Am J Pathol* 2015; 185: 651–665.
 55. Shen JS, Busch A, Day TS, et al. Mannose receptor-mediated delivery of moss-made alpha-galactosidase A efficiently corrects enzyme deficiency in Fabry mice. *J Inherit Metab Dis* 2016; 39: 293–303.
 56. Aerts JM, Groener JE, Kuiper S, et al. Elevated globotriaosylsphingosine is a hallmark of Fabry disease. *Proc Natl Acad Sci USA* 2008; 105: 2812–2817.
 57. Eglén RM, Hunter JC and Dray A. Ions in the fire: recent ion-channel research and approaches to pain therapy. *Trends Pharmacol Sci* 1999; 20: 337–342.
 58. Lumpkin EA and Caterina MJ. Mechanisms of sensory transduction in the skin. *Nature* 2007; 445: 858–865.
 59. Liguori R, Di Stasi V, Bugiardini E, et al. Small fiber neuropathy in female patients with Fabry disease. *Muscle Nerve* 2010; 41: 409–412.



Supplementary Fig. S1. Characterization of Capsaicin evoked ionic currents in DRG neurons of WT and α -GalA KO in cell culture. (a) Quantitative representation of TRPV1 Capsaicin activated DRG neurons – the percentage of all DRG neurons responding to 1 μ M Capsaicin stimuli was lower in α -Gal A(-/0) (35%) in comparison to its WT control (60%). The activation of TRPV1 currents is significantly diminished in α -Gal A(-/0) DRG neurons in comparison to WT. (b) Capacitance of Capsaicin responding cells – the DRG neurons responding to 1 μ M Capsaicin stimuli by activation of inward cationic currents showed no differences between α -Gal A(-/0) and α -Gal A(+/0) mice. (c) Quantitative representation of TRPV1 currents recorded at -60 mV during the time window of 72 hours. Values are given as means \pm SE; WT ($n_{24}=6$; $n_{48}=9$; $n_{72}=5$) and KO ($n_{24}=3$; $n_{48}=7$; $n_{72}=2$). (d) Quantitative assessment of TRPV1 currents density by normalization of peak current recorded at -60 mV to the capacitance of each cell. Values are given as means \pm SE; WT ($n_{24}=6$; $n_{48}=9$; $n_{72}=5$) and KO ($n_{24}=3$; $n_{48}=7$; $n_{72}=2$).



Supplementary Fig. S2. Long-term decrease in thermal sensitivity. (a) The statistically significant reduction in latency time of male KO group after administration of saline demonstrates higher acute sensitivity to noxious hot thermal stimulation than in male WT group after administration of saline ($p < 0.05$, $n = 14$ animals for WT, $n = 14$ animals for KO). (b) The subcutaneous administration of 3 mg/kg DD04107 peptide significantly reduced the thermal hypersensitivity produced in the α -Gal A (-/0) mouse model of FD ($n = 15$) by hot-plate stimulus of $52^{\circ}\text{C} \pm 0.1^{\circ}\text{C}$ in comparison to α -Gal A (-/0) KO mice injected with saline ($n = 14$) in different time points within 24 hours after the injection. Two-way ANOVA followed by Fisher's LSD post hoc test revealed that the peptide attenuated thermal nociception up to 24 hours post-administration (Genotype effect \times Time \times Treatment effect $F(6, 324) = 4.38$, $p = 0.0002$).